

# HyperMacs to HyperBlocks: A Novel Class of Branched Thermoplastic Elastomer

Lian R. Hutchings,<sup>\*,†</sup> Jonathan M. Dodds,<sup>†</sup> David Rees,<sup>†</sup> Solomon M. Kimani,<sup>†</sup> Jun Jie Wu,<sup>‡</sup> and Emily Smith<sup>‡</sup>

<sup>†</sup>Polymer IRC, Department of Chemistry, Durham University, Durham DH1 3LE, United Kingdom, and

<sup>‡</sup>School of Engineering, Durham University, Durham DH1 3LE, United Kingdom

Received August 14, 2009; Revised Manuscript Received October 2, 2009

**ABSTRACT:** We demonstrate here the great versatility of the macromonomer approach for the synthesis of long chain hyperbranched polymers (HyperMacs) and describe the synthesis of HyperMacs from polybutadiene and poly(methyl methacrylate) using analogous yet modified synthetic strategies. Furthermore, we report the synthesis, morphology, and mechanical properties of an entirely new class of HyperMacs—HyperBlocks—prepared from the coupling of polystyrene–polyisoprene–polystyrene triblock copolymer macromonomers. Transmission electron microscopy (TEM) studies show that these unconventional block copolymers undergo microphase separation, but the resulting morphologies lack any long-range order. Tensile testing shows that these materials offer promise as a new class of branched thermoplastic elastomer (TPE). Finally, blends of HyperBlock (10%) with a commercial linear TPE produced by Kraton show both enhanced ultimate tensile stress and elongation at break.

## Introduction

It is well understood that the physical properties of polymeric materials depend to a very large extent on the molecular architecture of the constituent polymeric chains. Variables such as molecular weight, molecular weight distribution, and the presence and degree of long-chain branching in polymers have huge implications for the solid and melt properties of a product. Over many years, the design and synthesis of well-defined molecular architectures such as star branched polymers,<sup>1–3</sup> mikto star polymers,<sup>4–6</sup> and H-shaped polymers<sup>7,8</sup> have contributed much to the understanding and prediction of the relationship between structure and properties. More recently, strategies have been devised to synthesize ever more complex, hierarchically, branched architectures with a variety of resulting structures and differing degrees of control over molecular structure. The various synthetic methodologies tend to result in polymers that can be divided into two categories. The first category might be described as well-defined long-chain branched analogues of dendrimers, with notable contributions from Hadjichristidis,<sup>9,10</sup> Gnanou,<sup>11–13</sup> Hedrick,<sup>14</sup> Hirao,<sup>15–19</sup> Monteiro,<sup>20–22</sup> and ourselves.<sup>23,24</sup> The primary aim of making such materials is to control all the molecular parameters, i.e., molecular weight and molecular weight distribution of the linear polymer between branch points and the degree and distribution of branching in the resulting branched architectures. However, in order to precisely control the structure of such materials, a synthetic strategy with many reaction and purification steps is required which results in very time-consuming synthesis and often yields relatively modest quantities of material.

The second category might similarly be described as the long-chain branched analogues of hyperbranched polymers in that the synthesis results in materials that are often polydisperse in both molecular weight and architecture. This category comprises many variations of branched structure with differing degrees of

structural homogeneity, and terms such as dendrigraft,<sup>25–28</sup> comb-burst,<sup>29</sup> arborescent,<sup>30</sup> hyperbranched,<sup>31</sup> and HyperMacs<sup>32</sup> have all been used to describe such polymers. Although these branched polymers all possess structural heterogeneity, the synthesis in all cases is relatively facile and economical and allows the production of useful quantities of materials. Noteworthy advances in this field include reports from Puskas on the synthesis of hyperbranched polyisobutylene by convergent cationic polymerization via a modified self-condensing vinyl polymerization.<sup>31</sup> Knauss et al. have synthesized a series of branched polystyrene polymers by a convergent method using anionic polymerization. This strategy allows the vinyl moiety in coupling agents like vinylbenzyl chloride (VCB), 4-(chlorodimethylsilyl)styrene (CDMSS),<sup>33,34</sup> and more recently 4-vinylstyrene oxide<sup>35</sup> to copolymerize with styrene while the chloromethyl, chlorosilane, and epoxide functionality react with the living carbanion to introduce branch points. Frey et al. recently adopted a facile macromonomer approach for the synthesis of highly branched polydienes.<sup>36,37</sup> Anionic polymerization of butadiene or isoprene was carried out in tetrahydrofuran (THF) to yield a low 1,4 microstructure and a large number of pendant vinyl groups. The living polymers were end-capped with chlorodimethylsilane to give an AB<sub>n</sub> type macromonomer. These macromonomers were then polymerized in the bulk by a hydrosilylation reaction using Karstedt's catalyst; however, the desired intermolecular coupling reactions were somewhat hampered by competing intramolecular cyclization reactions.

The concept of macromonomers, monomers that are macromolecular species containing polymerizable end groups, was first described by Milkovich,<sup>38</sup> who synthesized end-functionalized polymers by living anionic polymerization. Methods for the synthesis of highly branched polymer architectures using macromonomers as building blocks have subsequently been reported by a number of research groups including graft copolymers<sup>39</sup> and combs/star combs.<sup>40</sup> The advantage of the macromonomer approach in these strategies is the ability to control the molecular

\*Corresponding author. E-mail: l.r.hutchings@durham.ac.uk.

weight of the branches/combs independently from the backbone although there is still a certain lack of control in the molecular weight between branch points. The advantage of being able to independently control the molecular weight of the polymer between branch points has also been recognized and exploited in the synthesis of well-defined dendritically branched polymers by Monteiro,<sup>20–22</sup> who describes the synthesis of dendritically branched polymers prepared using a combination of atom transfer radical polymerization (ATRP) and click chemistry coupling reactions in a convergent coupling strategy. Linear polymers were prepared via ATRP and the appropriate groups (azide and alkyne) required for the click reaction introduced at the chain ends. This methodology beautifully demonstrates the “macromonomer” approach with the authors reporting branched polymers comprising of polystyrene and polyacrylate segments. However, ATRP undoubtedly places certain limitations on the molecular weight and polydispersity of the linear segments. The “macromonomer” approach adopted Frey and Monteiro is the strategy developed by ourselves several years ago for the synthesis of DendriMacs and HyperMacs in our contribution to this still growing area of polymer science. DendriMacs and HyperMacs are essentially long chain branched analogues of classical dendrimers and hyperbranched polymers, analogous in terms of both structure and mode of synthesis. Where dendrimers and hyperbranched polymers may be synthesized using low molecular weight AB<sub>2</sub> monomers, DendriMacs and HyperMacs are prepared from  $\alpha,\omega,\omega'$ -trifunctional AB<sub>2</sub> macromonomers—the macromonomers are coupled using a Williamson coupling reaction to afford the branched polymer.

As well as offering control over the molecular weight of the linear polymer sections in complex branched architectures, the other major advantage of the “macromonomer” approach is versatility. We have previously reported the synthesis of polystyrene<sup>23</sup> and polybutadiene<sup>24</sup> DendriMacs and the synthesis and the rheological characterization of polystyrene HyperMacs.<sup>32,41,42</sup> We report here the synthesis of polybutadiene and poly(methyl methacrylate) HyperMacs, both of which required modifications to the previously described strategies of varying degrees. We also describe the synthesis of an entirely new class of HyperMacs—HyperBlocks—constructed from macromonomers which are ABA triblock copolymers of polystyrene–polyisoprene–polystyrene (PS–PI–PS). PS–PI–PS triblock copolymers find extensive commercial use as thermoplastic elastomers, and we describe the results of investigations into the effect of the highly branched architecture upon both the solid-state morphology and mechanical properties of HyperBlocks. Intriguingly, when a sample of HyperBlock was blended with Kraton D1160—a commercially available linear PS–PI–PS triblock copolymer thermoplastic elastomer—a blend containing 10% HyperBlock showed both enhanced tensile stress and elongation at break in comparison to pure Kraton D1160.

## Experimental Section

**Materials.** Hexane (Aldrich, HPLC grade, >99%), benzene (Aldrich, HPLC grade, >99%), styrene (Aldrich, 99%), methyl methacrylate (Aldrich, 99%), and dichloromethane (in-house purification) were dried with calcium hydride (Aldrich), degassed by freeze–pump–thaw cycle, and freshly distilled in a vacuum line to the reaction vessel prior to use. Purification of 1,3-butadiene (Aldrich, >99%) was achieved by passing the monomer successively through columns of Carbosorb (Aldrich) and molecular sieves (Aldrich) to remove any inhibitor and moisture, respectively. *N,N,N',N'*-Tetramethylethylenediamine (Aldrich, >99.5%) and 3-(*tert*-butyldimethylsiloxy)-1-propyllithium in cyclohexane (InitiaLi 103, FMC corporation),

triphenylphosphine (Aldrich, 99%), and carbon tetrabromide (Aldrich) were used as received. 1,1-Bis(4-*tert*-butyldimethylsiloxyphenyl)ethylene was synthesized in two steps from dihydroxybenzophenone according to the procedure of Quirk and Wang.<sup>43</sup> Reagents for the Williamson coupling reaction, cesium carbonate, THF (anhydrous), DMF (anhydrous), and DMAc (anhydrous) were obtained from Aldrich and used as purchased. Two samples of commercial PS–PI–PS thermoplastic elastomers (D-1160 and D-1142P) were obtained from Kraton Polymers. Kraton D-1160 is a linear PS–PI–PS triblock copolymer with a styrene content of ca. 20%, while Kraton D-11245P is a star-branched PS–PI block copolymer with a styrene content of ca. 30%.

**Measurements.** Molecular weight analysis was carried out by size exclusion chromatography (SEC) on a Viscotek TDA 302 with refractive index (660 nm source), viscosity, and light scattering detector (with a 690 nm wavelength laser). A value of 0.124, 0.085, and 0.185 (obtained from Viscotek) was used for the  $dn/dc$  of polybutadiene, PMMA, and polystyrene, respectively. 2 × 300 mm PLgel 5  $\mu$ m mixed C columns (with a linear range of molecular weight from 200 to 2 000 000 g/mol) were used, and THF was used as the eluent with a flow rate of 1.0 mL/min at 35 °C. The extent of the coupling reactions was followed by SEC. <sup>1</sup>H NMR spectra were measured on either a Varian VNMRs 700 MHz, Varian Inova-500 MHz, or Bruker DRX-400 MHz spectrometer using either C<sub>6</sub>D<sub>6</sub> or CDCl<sub>3</sub> as solvents.

Samples for transmission electron microscopy (TEM) were cast from toluene solution (3% w/v) onto aluminum plates, dried at room temperature for 14 days, and then annealed at 393 K for 7 days to equilibrate the morphologies. Samples (TEM) were prepared by cryo-ultramicrotomy using a Leica EM UC6 ultramicrotome and a Leica EM FC6 cryochamber. Cryosections of 50–70 nm thickness were cut using a cryo 35° diamond knife at a temperature of –140 °C and then manipulated from the knife edge onto the grid. Sections were stained for 2–4 h with osmium tetroxide vapor and imaged with a Hitachi H7600 transmission electron microscope (Hitachi High Technologies Europe) using an accelerating voltage of 100 kV.

Tensile tests were carried out with dumbbell-shaped tensile specimens compression-molded at 160 °C for 18 min using a 10 ton heat press. An Instron 5565 universal material testing machine was used with an Instron 5 kN load cell at a testing temperature of 20 ± 1.5 °C. All specimens had a uniform initial cross-sectional area and gauge length between grips of 7.2 mm<sup>2</sup> and 20 mm, respectively. They were subjected to a constant nominal strain rate (0.01 s<sup>–1</sup>, cross-head speed of 12 mm/min). A pair of Instron self-tightening elastomer grips was used to prevent the specimen from slipping during tensile straining and to ensure good and consistent specimen alignment. Tensile tests were carried out on the sample of PS–PI–PS HyperBlock prepared in house as well as on two commercially available thermoplastic elastomers provided by Kraton Polymers, Kraton D-1160 and Kraton D-11245P. Blends of HyperBlock and Kraton D-1160 contain 10%, 20%, and 30% HyperBlock were also prepared and tested. The blends were prepared by solution blending in which the two polymers were codissolved in THF, stirred for 30 min after dissolution (to ensure mixing at a molecular level), and then recovered by precipitation into methanol. The recovered polymer blend was dried to constant mass in vacuo.

**Synthesis of AB<sub>2</sub> Macromonomers.** *Synthesis of Polybutadiene AB<sub>2</sub> Macromonomers.* Synthesis of all macromonomers was achieved using anionic polymerization using standard high-vacuum techniques. A typical synthesis of AB<sub>2</sub> polybutadiene macromonomer was as follows: *n*-hexane (100 mL) and butadiene (10 g, 0.092 mol) were distilled, under vacuum, into a 500 mL reaction flask. The required amount of 3-*tert*-butyldimethylsiloxy-1-propyllithium (0.7 M) in cyclohexane was injected to initiate the reaction through a septum—for a target *M<sub>n</sub>* of 6500 g mol<sup>–1</sup> 1.10 mL of initiator was added—and the

reaction mixture stirred for 4 days at room temperature to allow complete conversion. At the end of the reaction period, hexane and any traces of unreacted monomer were distilled out of the reaction vessel under vacuum and replaced with fresh dry hexane. A small sample was then removed and terminated with nitrogen-sparged methanol for molecular weight and NMR analysis. In a separate flask 1,1-bis(4-*tert*-butyldimethylsiloxyphenyl)ethylene (fDPE) (1.5 mol equiv with respect to initiator) was azeotropically dried with benzene, before addition of dry hexane and TMEDA (2.0 equiv with respect to initiator). The fDPE/TMEDA solution was further purified by the dropwise addition of *sec*-butyllithium until a persistent red color was observed. The purified fDPE solution was added to the living polymer solution. The end-capping reaction was stirred for 5 days at room temperature prior to being terminated with nitrogen-sparged methanol. The polymer was recovered by precipitation in methanol and dried in vacuo. The protected alcohol functionalities on the product were deprotected using 10 M HCl (10:1 molar ratio with respect to the macromonomer) in THF (10% w/v) under reflux for 24 h, and the polymer was recovered by precipitation in methanol and dried. The primary alcohol end group was converted into an alkyl bromide according to a previously described method.<sup>41</sup> The purified material was precipitated into methanol and dried to a constant mass.  $M_n = 6500 \text{ g mol}^{-1}$ ,  $M_w = 7100 \text{ g mol}^{-1}$ , PDI = 1.07. <sup>1</sup>H NMR (400 MHz, C<sub>6</sub>D<sub>6</sub>). Protected polybutadiene:  $\delta$  7.0 (Ar), 6.5 (Ar), 5.6–5.4 (=CH), 5.0 (=CH vinyl), 3.94 (CH<sub>2</sub>OPh), 3.76 (HC(Ph)<sub>2</sub>), 3.56 (CH<sub>2</sub>OSi), 1.0 (Si(CH<sub>3</sub>)<sub>2</sub>C(CH<sub>3</sub>)<sub>3</sub>), 0.1 (ArOSi(CH<sub>3</sub>)<sub>2</sub>C(CH<sub>3</sub>)), 0.0 (CH<sub>2</sub>OSi(CH<sub>3</sub>)<sub>2</sub>C(CH<sub>3</sub>)<sub>3</sub>). Deprotection polybutadiene:  $\delta$  3.94 (Ph–OH), 3.76 (HC(Ph)<sub>2</sub>), 3.35 (CH<sub>2</sub>OH). Brominated polybutadiene:  $\delta$  2.97 (CH<sub>2</sub>Br).

**Synthesis of Poly(methyl methacrylate) AB<sub>2</sub> Macromonomers.** Poly(methyl methacrylate) (PMMA) AB<sub>2</sub> macromonomer was synthesized using an initiator prepared in situ by the reaction of fDPE with *sec*-BuLi. A typical reaction was as follows: for a target molecular weight of 10 000 g mol<sup>−1</sup> fDPE (0.882 g, 2 mmol) and LiCl (0.212 g, 5 mmol) were added to the reaction vessel, and air was evacuated before the mixture was azeotropically dried with benzene. 100 mL of dry THF was added, and the solution cooled to −78 °C, followed by the dropwise addition of *sec*-BuLi until a persistent red color was observed. This procedure was carried out to remove any traces of impurities. To the purified fDPE solution was added *sec*-BuLi (0.83 mL of 1.2 M solution), and the solution was left to stir overnight to generate the fDPE initiator. To the deep red solution was added dry methyl methacrylate (MMA) (10.68 g, 0.11 mol) using an airtight-lockable syringe via a rubber septum at a rate of ~1 mL/min. Upon addition of the monomer, the deep red color of the initiating species turned pale yellow. The reaction was stirred at −78 °C for 24 h at which point 2.03 mL (0.02 mol) of freshly distilled 1,3-dibromopropane was added to the living polymer solution (still at −78 °C) through a septum. The reaction mixture was stirred and allowed to warm very slowly to room temperature over a period of several hours. Any unreacted living polymer was quenched with nitrogen-sparged methanol, and the polymer was recovered by precipitation in ice cold methanol. The *tert*-butyldimethylsilyl (TBDMS) protecting groups at the initiating end of the polymer chain were converted into phenol groups by mild acid hydrolysis, as described earlier for polybutadiene, to give a PMMA AB<sub>2</sub> macromonomer.  $M_n = 11\,200 \text{ g mol}^{-1}$ , PDI = 1.05. <sup>1</sup>H NMR (400 MHz, C<sub>6</sub>D<sub>6</sub>). Protected PMMA:  $\delta$  7.14–7.06 (Ar–H), 3.45–3.28 (OCH<sub>3</sub>), 2.87 (CH<sub>2</sub>Br), 2.24–2.00 (CH<sub>2</sub>), 1.36–1.19 (CH<sub>3</sub>), 1.01 (Si(CH<sub>3</sub>)<sub>2</sub>C(CH<sub>3</sub>)<sub>3</sub>), 0.15 (Si(CH<sub>3</sub>)<sub>2</sub>C(CH<sub>3</sub>)<sub>3</sub>).

**Synthesis of Poly(styrene–isoprene–styrene) (PS–PI–PS) Triblock AB<sub>2</sub> Macromonomer.** Benzene (500 mL) and styrene (8.65 g, 0.08 mol) were distilled, under vacuum, into a 1 L reaction flask. To the monomer solution 3-*tert*-butyldimethylsiloxy-1-propyllithium (0.4 M in cyclohexane) was injected through a rubber septum. For a target  $M_n$  of 10 000 g mol<sup>−1</sup>

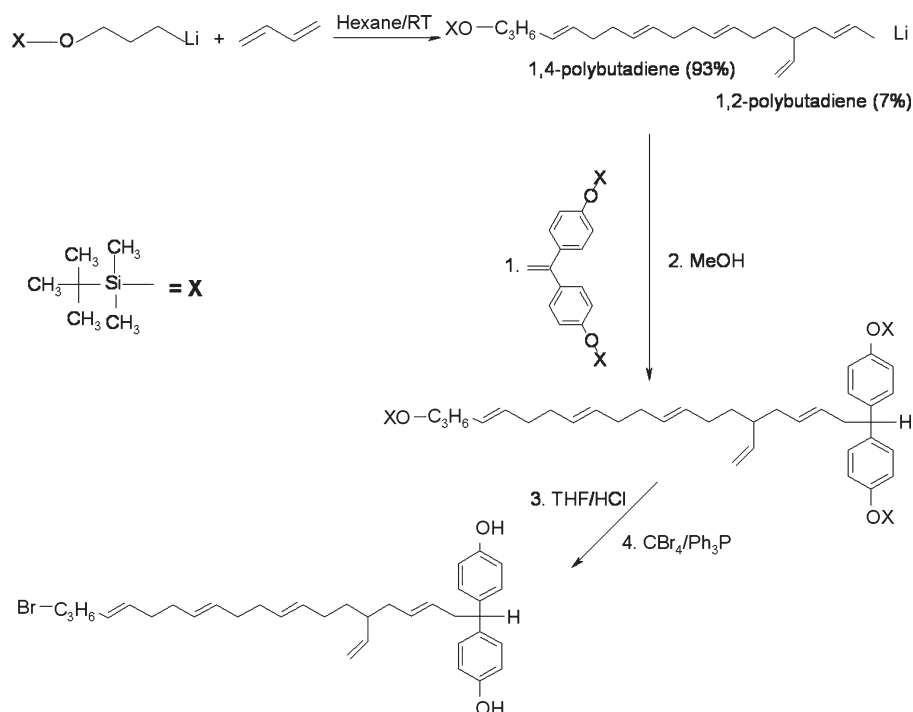
(PS block 1), 1.78 mL of initiator (7 mmol) was used. Upon addition of the initiator to the reaction mixture, a pale yellow color was observed which evolved over a period of time into the orange-red color of living polystyryllithium. The solution was stirred overnight at room temperature to allow complete consumption of styrene monomer before a small sample was removed for molecular weight and NMR analysis. To the living polymer solution, isoprene (29.20 g, 0.43 mol, PI block target  $M_n = 40\,000 \text{ g mol}^{-1}$ ) was added, resulting in a colorless solution, and the mixture was stirred for 3 days at room temperature to ensure complete conversion. TMEDA (0.11 mL, 7 mmol) was added prior to the second batch of styrene (9.15 g, 0.87 mol for a PS block target  $M_n = 10\,000 \text{ g mol}^{-1}$ ) to ensure rapid reinitiation: addition of styrene to the living solution regenerating the orange-red color of polystyryllithium. The reaction was left to stir at room temperature for 3 h before the addition of purified 1,1-bis(4-*tert*-butyldimethylsiloxyphenyl)ethylene (1.5 mol equiv with respect to lithium) as a solution in benzene, which was then stirred at room temperature for a further 5 days before the reaction was terminated with nitrogen-sparged methanol. The protected AB<sub>2</sub> PS–PI–PS macromonomer was recovered by precipitation in methanol, redissolved in benzene, reprecipitated once more into methanol, and dried in vacuo. The *tert*-butyldimethylsilyl (TBDMS) protecting groups at the initiating and the terminating end of the polymer chain were converted into an alcohol and two phenol groups, respectively, by mild acid hydrolysis (as described above) to yield the deprotected AB<sub>2</sub> macromonomer. The primary alcohol end group was converted into an alkyl bromide as previously described. PS block  $M_n = 14\,600 \text{ g mol}^{-1}$ , PDI = 1.45. PS–PI block  $M_n = 34\,600 \text{ g mol}^{-1}$ , PDI = 1.18. PS–PI–PS block  $M_n = 46\,100 \text{ g mol}^{-1}$ , PDI = 1.18. <sup>1</sup>H NMR (500 MHz, C<sub>6</sub>D<sub>6</sub>). Protected PS–PI–PS macromonomer:  $\delta$  3.36 (CH<sub>2</sub>OSi), 3.5 (HC(Ph)<sub>2</sub>), 1.0 (Si(CH<sub>3</sub>)<sub>2</sub>C(CH<sub>3</sub>)<sub>3</sub>), 0.1 (ArOSi(CH<sub>3</sub>)<sub>2</sub>C(CH<sub>3</sub>)), 0.0 (CH<sub>2</sub>OSi(CH<sub>3</sub>)<sub>2</sub>C(CH<sub>3</sub>)<sub>3</sub>). Deprotected PS–PI–PS macromonomer:  $\delta$  3.15 (CH<sub>2</sub>OH), 3.7–3.8 (HO–Ph). Brominated PS–PI–PS macromonomer: 2.75 (CH<sub>2</sub>Br).

**HyperMac and HyperBlock Synthesis.** Coupling reactions of the AB<sub>2</sub> macromonomers were carried out under an inert atmosphere via Williamson ether formation using cesium carbonate as a base. The choice of solvent and the solution concentration varied depending on the macromonomer. Coupling reactions for the polybutadiene macromonomer were carried out in a mixed solvent system composed of *N,N*-dimethylacetamide (DMAc) and tetrahydrofuran (THF) in a ratio of 1:1. Typically, 1.00 g of the macromonomer ( $M_n = 6500 \text{ g mol}^{-1}$ , 0.035 mmol), cesium carbonate (0.095 g, 0.292 mmol), and 10 mL of THF/DMAc (1:1) were added to a flask fitted with a mechanical stirrer and reflux condenser. The mixture was vigorously stirred at 60 °C, and the progress was monitored by size exclusion chromatography by sampling at timed intervals until no further increase in molecular weight was observed. The mixture was then allowed to cool to room temperature, and the product was recovered by precipitation into methanol that contained 2% BHT antioxidant. The product was redissolved in THF and reprecipitated once again in methanol before drying. A similar approach was used to couple PMMA macromonomers using DMF as the solvent (20% w/v) and to couple PS–PI–PS macromonomers in THF/DMF (1:1) as the solvent (10% w/v).

## Results and Discussion

In a series of previous papers,<sup>32,41,42</sup> we have described the synthesis (and improved synthesis) of polystyrene HyperMacs. The synthesis takes place in two steps: the first step involves the preparation of the macromonomers—the linear building blocks of the branched polymer—by living anionic polymerization, and the second step involves coupling of the linear macromonomers to form the highly (if randomly) branched HyperMacs. This two-step strategy offers a number of distinct advantages. First, living



Scheme 1. Synthesis of AB<sub>2</sub> Polybutadiene Macromonomer

anionic polymerization offers maximum control over the molecular weight and polydispersity of the linear sections between branch points, and second, the decoupling of the two processes—polymerization and coupling/branching—offers the possibility to make and subsequently couple a wide variety of macromonomers and in particular well-defined block copolymeric macromonomers. Having optimized this two-step strategy using polystyrene as an example, we can now demonstrate the versatility of the “macromonomer” approach by describing the synthesis of HyperMacs made from polybutadiene, PMMA, and block copolymers of polystyrene/polyisoprene. The use of well-defined PS–PI–PS block copolymers as building blocks results in highly branched block copolymer (HyperBlocks) which have the potential to be a new class of branched thermoplastic elastomer (TPE), and we will describe preliminary results of investigations into the effect of the branched architecture upon the solid state morphology and mechanical properties

**Polybutadiene Macromonomers.** The synthesis of the polybutadiene AB<sub>2</sub> macromonomers requires only minor modifications to the described method for the synthesis of polystyrene macromonomers.<sup>32,41</sup> The polymerization proceeded in *n*-hexane (to maintain a high 1,4 microstructure) and was initiated using the commercially available lithium initiator, 3-*tert*-butyldimethylsiloxy-1-propyllithium, which contains a protected alcohol (A) functionality. Introduction of the two phenol (B) functionalities was achieved by end-capping the living polymer with the functionalized diphenylethylene derivative 1,1-bis(4-*tert*-butyldimethylsiloxyphenyl)ethylene (fDPE) which contains two protected phenol functionalities (see Scheme 1). In contrast to the reaction of fDPE with polystyryllithium, TMEDA ([TMEDA]/[PBDLi] = 2) was added to promote the end-capping reaction. The addition of PBDLi to DPE in hydrocarbon solvents has been shown by Quirk and Lee to be slow to the point of being impractical.<sup>44</sup> However, the addition of a Lewis base results in the dissociation of PBDLi aggregates, resulting in PBDLi species that are more reactive toward addition to DPE. Although sufficient time was allowed for complete consumption of the all the butadiene monomer, as a safety precaution

any (potential) residual monomer was removed before addition of DPE. The reactivity of the living diphenylethyllithium end group toward butadiene is high, and this could lead to the introduction of multiple DPE groups within a polymer chain. The removal of any potential monomer was achieved by distillation under vacuum, of the polymerization solvent, removing any residual monomer at the same time; fresh, dry solvent was subsequently distilled into the reaction vessel. To ensure that the end-capping reaction was quantitative, the reaction was stirred for 5 days at room temperature, after which the polymer was terminated with degassed methanol and the product precipitated in methanol. The <sup>1</sup>H NMR (CDCl<sub>3</sub>) spectra of the methanol quenched PBD–DPE adduct showed signals at 6.8 and 7.15 ppm, which were assigned to the aromatic ring while the CH<sub>3</sub>–Si protons of the protecting group introduced by the end-capping reaction and the initiator were observed at 0.17 and 0.04, respectively. Integration of the signals corresponding to the terminal methine hydrogen Ph<sub>2</sub>H (δ 3.85 ppm) to CH<sub>2</sub>OSi from the initiator residue (δ 3.60 ppm) showed that ~90% of the polymer chains had been successfully end-capped with fDPE. In situations where residual monomer was not removed prior to the end-capping reaction, NMR indicated that the ratio between the terminal methine hydrogen (Ph<sub>2</sub>H) and the CH<sub>2</sub>OSi was less than 50%, whereas the integration of the CH<sub>2</sub>OSi with respect to the aromatic protons of fDPE suggested that the ratio of fDPE units to initiating moieties was ~0.9. This tends to support the assertion that any residual traces of butadiene monomer present upon addition of the fDPE could copolymerize with the fDPE, introducing more than one fDPE unit into some chains while leaving other chains devoid of fDPE—clearly a situation which has implications for the efficiency of subsequent coupling reactions. The TBDMS (alcohol) protection groups were removed by a mild acid hydrolysis, and the primary alcohol moiety converted to an alkyl bromide functionality using CBr<sub>4</sub>/PPh<sub>3</sub> to give an AB<sub>2</sub> macromonomer. These end-group modification reactions were followed by <sup>1</sup>H NMR (C<sub>6</sub>D<sub>6</sub>) where the signal corresponding to

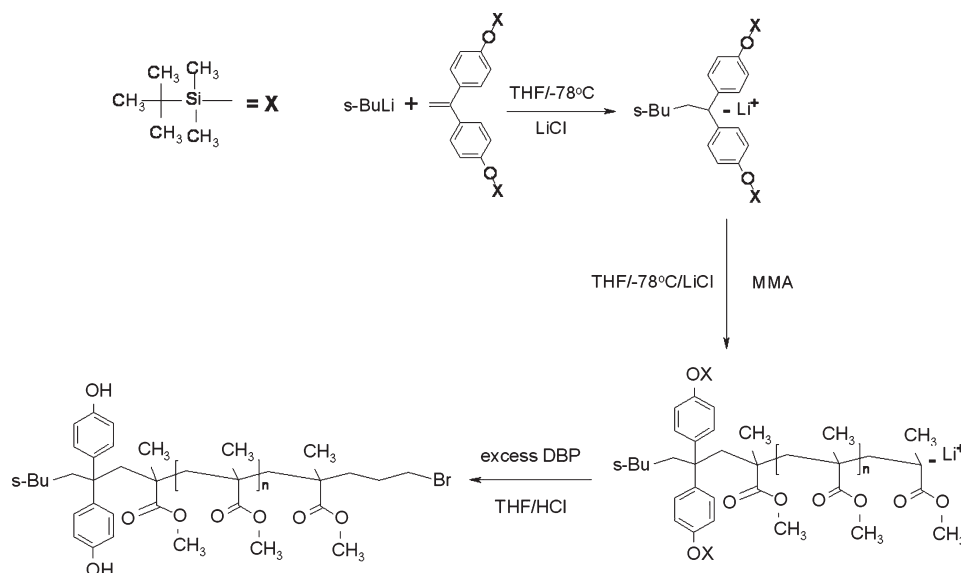
Scheme 2. Synthesis of AB<sub>2</sub> PMMA Macromonomer

Table 1. Effect of Time, Temperature, and Molar Ratio of Dibromopropane (DBP) to Living PMMA Chain Ends ([DBP]/[Li]) on the Degree of End-Capping of PMMA by DBP

sample	target MW/g mol <sup>-1</sup>	[DBP]/[Li]	temp	time/h	M <sub>n</sub> /g mol <sup>-1</sup>	PDI	% Br
1 <sup>a</sup>	10 000	20	-78 °C	72	9 200	1.04	67
2 <sup>a</sup>	5 000	20	-78 °C	96	5 500	1.07	76
3 <sup>b</sup>	10 000	20	-78 °C → RT <sup>c</sup>	72	11 200	1.04	63
4 <sup>b</sup>	10 000	40 <sup>d</sup>	-78 °C → RT <sup>c</sup>	72	30 500	1.04	97 <sup>d</sup>
5 <sup>b</sup>	5 000	40	-78	72	4 900	1.14	84

<sup>a</sup> Initiator formed by reaction of diphenylethylene and *s*-BuLi. <sup>b</sup> Initiator formed by reaction of 1,1-bis(4-*tert*-butyldimethylsiloxyphenyl)ethylene and *s*-BuLi. <sup>c</sup> DBP added at -78 °C and then reaction temperature warmed to room temperature over 72 h. <sup>d</sup> Since actual molecular weight is significantly higher than target molecular weight, the effect ratio of [DBP]/[Li] will also be much higher than 40:1.

CH<sub>2</sub>-X of the initiating moiety shifted from  $\delta$  3.56 ppm (X = OTBDMS) to 3.35 ppm (X = OH) to 2.97 ppm (X = Br). Also observed was the complete disappearance of the phenol protection groups and the subsequent emergence of the PhOH ( $\delta$  3.94). Two polybutadiene macromonomers were prepared: PB1 with a number-average molar mass of 6500 g mol<sup>-1</sup> and a PDI of 1.09 and PB2 with a number-average molar mass of 15 750 g mol<sup>-1</sup> and a PDI of 1.04.

**Synthesis of Poly(methyl methacrylate) AB<sub>2</sub> Macromonomers.** The anionic polymerization of methyl methacrylate is somewhat more complicated than that of polystyrene or the dienes, and initiation with simple alkyl lithium species does not lead to well-defined polymers.<sup>45</sup> In order to prevent attack by the initiator on the carbonyl group on the monomer, the use of a sterically bulky initiator is required. Although this means that major modifications to the synthetic methodology for macromonomer synthesis are required, these modifications are easily achieved. The requirement for a bulky initiator was fulfilled by the use of a 1,1-diphenylalkyllithium species that was obtained by the in situ reaction between fDPE and *sec*-BuLi as shown in Scheme 2. This serves not only to meet the requirements for a bulky initiator but also results in the simultaneous introduction of the desired two phenol (B) groups at the chain end. Synthesis of the bulky functionalized initiator was carried out in THF at -78 °C. Butyllithium was added dropwise to a solution of fDPE in THF under a nitrogen atmosphere until the red color of diphenylhexyllithium persists. This process is carried out to "titrate" out any residual impurities. If impurities remain, the addition of BuLi results in reaction with the impurities. When all the impurities have been consumed, the next drop of initiator reacts with fDPE and

forms a pale red color. If this color remains, then the system is now free of impurities. At this point the desired amount of initiator required for the polymerization was added; the reaction between *sec*-BuLi and fDPE was allowed to proceed overnight. Methyl methacrylate monomer was subsequently introduced to the reaction vessel and propagation proceeded (in the presence of LiCl to control the molecular weight distribution)<sup>45</sup> for 24 h at -78 °C. The living polymer chains were end-capped with 1,3-dibromopropane (DBP) to introduce an alkyl bromide functionality at the chain end—a large excess of DBP was added to inhibit chain coupling between macromonomers. A series of experiments were carried out to optimize this end-capping reaction (see Table 1). The anionic polymerization of PMMA must be carried out at low temperatures to prevent termination via a backbiting reaction,<sup>45</sup> and end-capping reactions must also be carried out at these low temperatures. <sup>1</sup>H NMR (C<sub>6</sub>D<sub>6</sub>) analysis indicated a broad signal at 2.87 ppm corresponding to CH<sub>2</sub>Br—introduced as a result of the end-capping reaction. A comparison of the integral of this peak with either the aromatic protons or TBDMS protons on the initiator moiety enabled a calculation to determine the degree of end-capping, i.e., the number of chains successfully functionalized. Results shown in Table 1 show that increasing the end-capping reaction time from 72–96 h resulted in a modest improvement in the degree of functionalization, as did allowing the reaction temperature to rise slowly to room temperature over the duration of the reaction. However, increasing the stoichiometric ratio of DBP with respect to living chain ends appears to have the greatest impact on the degree of functionalization with a value of 84% for a [DBP]/[Li] of 40:1. A nearly quantitative extent of end-capping was achieved in experiment 4;

**Table 2. Molecular Weight, Polydispersity, and Composition Data for PS–PI–PS AB<sub>2</sub> Macromonomer<sup>a</sup>**

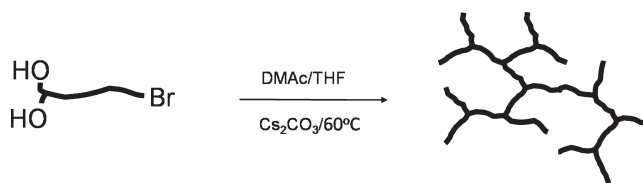
sample	$M_n$ (g mol <sup>-1</sup> ) <sup>b</sup>	$M_n$ (g mol <sup>-1</sup> ) <sup>c</sup>	$M_n$ (g mol <sup>-1</sup> ) <sup>d</sup>	PDI
PS	14 600	14 600	14 600	1.45
PS–PI	53 200 (38 600)	34 600 (20 000)	44 000 (29 400)	1.18
PS–PI–PS	64 100 (10 900)	46 100 (11 500)	55 000 (11 000)	1.18

<sup>a</sup> Total polystyrene content = 40 wt % according to <sup>1</sup>H NMR. Figure in parentheses corresponds to data for the additional block. <sup>b</sup> PS data obtained by triple detection SEC in THF using a value of  $dn/dc$  of 0.185. The SEC value for the molecular weight of PS used to calculate  $M_n$  of subsequent blocks by <sup>1</sup>H NMR. <sup>c</sup> Data obtained by triple detection SEC in THF using a value of  $dn/dc$  of 0.185 for each sample. <sup>d</sup> Data obtained by triple detection SEC in THF using values of  $dn/dc$  calculated using weight fractions of PS and PI obtained by <sup>1</sup>H NMR assuming a  $dn/dc$  for PS = 0.185 and  $dn/dc$  for PI of 0.130; therefore  $dn/dc$  PS–PI and PS–PI–PS calculated to be 0.145 and 0.152, respectively.

however, since the actual molecular weight of the resulting polymer was 3 times the intended molecular weight (likely due to the presence of traces of impurities), the effective ratio of [DBP]/[Li] is certain to be much higher than 40:1 and is possibly as high as 120:1. The large excess of unreacted DBP was easily removed by repeated precipitation of the polymer into cold methanol from THF. <sup>1</sup>H NMR analysis confirmed that the TBDMS protecting groups were successfully removed by acid hydrolysis to give an AB<sub>2</sub> poly(methyl methacrylate) macromonomer without affecting the ester functionalities on the polymer backbone. Three PMMA macromonomers were prepared: PMMA1, PMMA2, and PMMA3 (samples 3, 4, and 5 in Table 1) with  $M_n$  of 11 200, 30 900, and 4900 g mol<sup>-1</sup>, respectively.

**Polystyrene–Polyisoprene–Polystyrene (PS–PI–PS) Macromonomers.** Synthesis of the AB<sub>2</sub> PS–PI–PS macromonomer followed essentially the same strategy as that described above for the synthesis of polybutadiene macromonomers. The polymerization of the first PS block was initiated with 3-*tert*-butyldimethylsiloxy-1-propyllithium. The block copolymer was then prepared by sequential addition of isoprene and then styrene with the addition of TMEDA before the addition of the final batch of styrene to ensure rapid initiation of the styrene by polyisoprenyllithium. Introduction of the two phenol (B) functionalities was achieved in an identical fashion to that carried in the case of polybutadiene macromonomers, namely, by end-capping the living polymer with the functionalized diphenylethylene derivative 1,1-bis(4-*tert*-butyldimethylsiloxyphenyl)ethylene (fDPE). <sup>1</sup>H NMR indicated that the degree of end-capping was similar to that in previous cases with ~90% of the polymer chains successfully end-capped. Deprotection of the alcohol groups with mild acid hydrolysis followed by bromination of the primary alcohol group yields the AB<sub>2</sub> PS–PI–PS macromonomer. A combination of <sup>1</sup>H NMR and SEC was used to establish the molecular weight and composition of the resulting triblock copolymer, and the data are shown in Table 2.

It can be seen from the data in Table 2 that the polydispersity of the initial PS block is not narrow (1.45). This is to be expected since the initiator is an *n*-alkyl species, and these are known to be less efficient initiators due to higher degrees of aggregation—a phenomenon we observed in a previous paper describing the synthesis of polystyrene HyperMacs.<sup>32</sup> To alleviate this problem in previous studies, a small quantity of TMEDA was added to disaggregate the initiator, and narrow molecular weight distributions resulted. However, in the case of PS–PI–PS macromonomers it was decided to omit the addition of TMEDA in order to avoid any significant alteration to the highly desirable 1,4

**Scheme 3. Schematic Representation of the Synthesis of Polybutadiene HyperMac from AB<sub>2</sub> Polybutadiene Macromonomer**

enchainment of the polyisoprene block—hence the high value of PDI for the PS block. As expected, the addition of subsequent batches of monomer resulted in a narrowing of the PDI, confirming that this is a problem associated with the initiation step. There are three sets of molecular weight data in Table 2. In all cases the molecular weight of the PS block was analyzed by triple detection SEC, and we have absolute confidence in this value. The values for the PS–PI and PS–PI–PS samples in the first column were obtained by <sup>1</sup>H NMR—by comparing the integrals of signature peaks from PI and PS. The molecular weight data in the second column were obtained using triple detection SEC using a value for  $dn/dc$  of 0.185 for each sample. This is the  $dn/dc$  of polystyrene, and this data are merely qualitative. The data in the final column were also obtained using triple detection SEC, but a value of  $dn/dc$  for each sample was calculated using the weight fraction of each polymer (obtained by <sup>1</sup>H NMR) and the  $dn/dc$  for each homopolymer. The value of 0.185 for polystyrene was obtained from Viscotek (the SEC manufacturer) and is a value we have verified internally on many occasions. The value used for polyisoprene (0.130) was obtained from two independent sources in the literature.<sup>46,47</sup> It should be noted that the agreement between the molecular weights obtained by NMR and SEC is reasonable but not great, and the disagreement appears to arise predominantly from differences in the polyisoprene block molecular weight. It is not immediately obvious why this discrepancy arises. The NMR data are in good agreement with the predicted molar masses for each block (10–40–10) so perhaps the value for the  $dn/dc$  for PI is the source of the inaccuracy. The literature values were obtained with a 633 nm laser at unreported temperatures. The value of  $dn/dc$  for a polymer is very sensitive to a number of parameters including the wavelength of laser, solvent, and temperature. Any overestimation of the value of the  $dn/dc$  of polyisoprene will decrease the calculated value for the molecular weight. A further possible source of inaccuracy arises from the fact that there will be a distribution of composition in the block copolymers due to the inherent polydispersity of the sample, which in turn will result in a distribution of  $dn/dc$  values.

**Synthesis of HyperMacs.** We have previously described<sup>32,41</sup> a synthetic strategy for the production of polystyrene HyperMacs from AB<sub>2</sub> polystyrene macromonomers. This involves coupling the macromonomers via a Williamson etherification reaction, and this coupling reaction was optimized considering the effect of solvent, base, leaving group, temperature, and macromonomer solution concentration. Under optimal conditions, 20% w/v solution in DMF at 40 °C with cesium carbonate as the base and bromine as the leaving group, the extent and efficiency of the coupling reaction were such that very highly branched, high molecular polymers were produced in a matter of a few hours—much quicker if higher temperatures were used. We report here the results of investigations into the required modifications to allow the synthesis of HyperMacs from polybutadiene, PMMA, and PS–PI–PS block copolymers.

**Table 3. Molecular Weight, Polydispersity, and Intrinsic Viscosity Data for the Synthesis of Polybutadiene HyperMac from PB2 ( $M_n$  15 750  $\text{g mol}^{-1}$ ) after Various Times<sup>a</sup>**

time/h	$M_n$ ( $\text{g mol}^{-1}$ )	$Dp_n$	$M_w$ ( $\text{g mol}^{-1}$ )	$Dp_w$	PDI	$[\eta]_{\text{hyper}}/\text{dL g}^{-1}$ <sup>b</sup>	$[\eta]_{\text{lin}}/\text{dL g}^{-1}$ <sup>c</sup>	$g'^d$
1	36 000	2.3	76 600	4.7	2.10	1.05	1.053	0.99
2	74 000	4.7	229 400	14.0	3.10	1.25	2.38	0.52
3	163 600	10.4	672 700	41.0	4.10	1.80	5.27	0.34
4	184 900	11.7	648 900	40.2	3.50	1.82	5.14	0.35
6	188 400	12.0	692 500	42.2	3.70	2.12	5.39	0.39

<sup>a</sup> Coupling reaction carried out at 60 °C, 50:50 DMAc/THF. <sup>b</sup> Measured by SEC viscometry. <sup>c</sup> Calculated using the Mark–Houwink equation  $[\eta] = KM^a$ . <sup>d</sup>  $g' = [\eta]_{\text{hyper}}/[\eta]_{\text{linear}}$ .

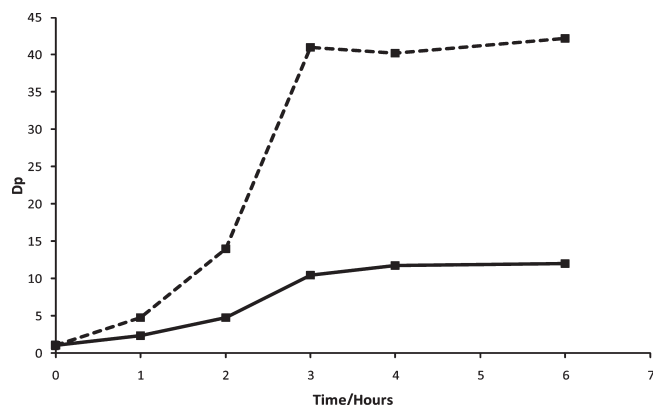


**Figure 1.** Evolution of  $Dp_n$  (solid line) and  $Dp_w$  (dashed line) with time for synthesis of polybutadiene HyperMac from PB2 ( $M_n$  15 750  $\text{g mol}^{-1}$ ). Coupling reaction carried out at 60 °C, 50:50 DMAc/THF.

**Polybutadiene HyperMacs.** Williamson coupling reactions are promoted by the use of aprotic solvents with high dielectric constants, and the successful coupling of polystyrene macromonomers was achieved in DMF.<sup>32,41</sup> However, polybutadiene is not soluble in DMF or other potentially useful solvents such as dimethylacetamide (DMAc). While polybutadiene is soluble in THF—another possible candidate solvent—we have previously shown that coupling reactions in THF proceed very slowly, probably due to the much lower dielectric constant compared to DMF (7.58 and 36.71 for THF and DMF at 25 °C, respectively). Investigations in a parallel study into the synthesis of polybutadiene DendriMacs<sup>24</sup> demonstrated that a mixed solvent of DMAc and THF (50/50 v/v) had sufficient solubility for the polybutadiene macromonomer and a high enough dielectric constant to allow the coupling reactions to proceed efficiently. However, it was also noted that that diluting the high dielectric solvent with THF reduced the rate of reaction, and the polybutadiene coupling reactions proceeded more slowly than analogous reactions of polystyrene macromonomers in DMF. Hence, polybutadiene macromonomer coupling reactions were carried out at 60 °C (cf. 40 °C for polystyrene macromonomers in DMF). Scheme 3 depicts a schematic representation of the HyperMac synthesis although it should be remembered that the resulting HyperMacs are polydisperse in terms of both molecular weight and architecture. We find it most convenient to describe the extent of the coupling reaction in terms of the degree of polymerization,  $Dp$ , where  $Dp$  describes the degree of macromonomer polymerization, i.e., how many macromonomers have reacted in forming the HyperMac. Hence,  $Dp_n$  is  $M_n(\text{HyperMac})/M_n(\text{macromonomer})$  and similarly  $Dp_w$  is  $M_w(\text{HyperMac})/M_w(\text{macromonomer})$ . As  $AB_2$  coupling reactions of this type proceed,  $M_w$  and therefore  $Dp_w$  increases more rapidly than  $M_n$  and therefore  $Dp_n$ . It can be seen from the data in Table 3 and Figure 1 that the coupling reactions appear to proceed in three distinct phases. The first phase is characterized by a

modest increase in  $Dp_w$  and lasts for the first hour. After 1 h the  $Dp_w$  begins to increase at a much higher rate; this second phase lasts for a relatively short period of time and is followed after 3 h by a third and final phase in which the rate of increase in molecular weight seems to plateau. This behavior is consistent with our previous observations.<sup>41</sup> We believe that during the first phase reaction occurs initially between individual macromonomers and then between macromonomers and HyperMacs comprised of only a few macromonomers. The onset of the rapid increase in molecular weight observed in phase two (between 2 and 3 h) arises predominantly via the coupling of HyperMac to HyperMac, eventually resulting in the presence of a significant proportion of very high molecular weight species. The emergence of the “super” HyperMacs toward the end of the second phase can be seen in the SEC chromatograms (Figure 2). The SEC chromatogram recorded after 1 h indicates that there is still a significant amount of uncoupled macromonomer—as evidenced by the sharp peak with a retention volume of about 14.0 mL—as well as well as dimer and trimer with peaks at lower elution volumes. The SEC chromatogram obtained after 2 h corresponds to a point in the reaction where the rate of increase of  $Dp_w$  is starting to rise dramatically (see Figure 1). It can be seen that the relative intensity of the peak at 14.0 mL corresponding to unreacted macromonomer has diminished significantly, indicating further macromonomer has been consumed, and the main broad peak maximum is to be found at about 12.0 mL. After 3 h the reaction appears to approaching completion as evidenced by the emerging plateau in Figure 1. At this point the  $Dp_w$  is in excess of 40 and has a weight-average molecular weight of close to 700 000  $\text{g mol}^{-1}$ . The very rapid increase between 2 and 3 h occurs we believe as a result of the coupling of HyperMac to HyperMac. The emergence of a shoulder to lower elution volumes (between 9 and 10 mL) can be observed in the SEC chromatogram collected after 3 h, indicating the presence of a significant proportion of the very high molecular weight “super” HyperMacs. The data in Figure 1 suggest that after 3 h the coupling reaction is into the final phase where the high molecular weight leads to very high solution viscosities, making efficient stirring/mixing a limitation. It is likely that reaction of the diminishing number of reactive “A” functionalities becomes diffusion controlled and the rate of reaction drops, resulting in the plateau that defines the third phase of the coupling reaction.

Values of  $g'$ , the branching factor, were calculated, and the data are shown in Table 3,  $g'$  being given by the ratio of the intrinsic viscosity of the branched polymer  $[\eta]_{\text{hyper}}$  to the intrinsic viscosity of a linear polymer  $[\eta]_{\text{linear}}$  of the same molecular weight.<sup>16</sup> Shown in Table 3 is the development of intrinsic viscosity of the HyperMac,  $[\eta]_{\text{hyper}}$ , with time and the intrinsic viscosity of a series of linear polymers of the same  $M_w$ . The intrinsic viscosity of the linear polymers was calculated using the Mark–Houwink equation with values of  $a = 0.74$  and  $K = 25.6 \times 10^{-5} \text{ dL/g}$  (sourced from *Polymer Handbook*<sup>48</sup>). Branched polymers have a smaller



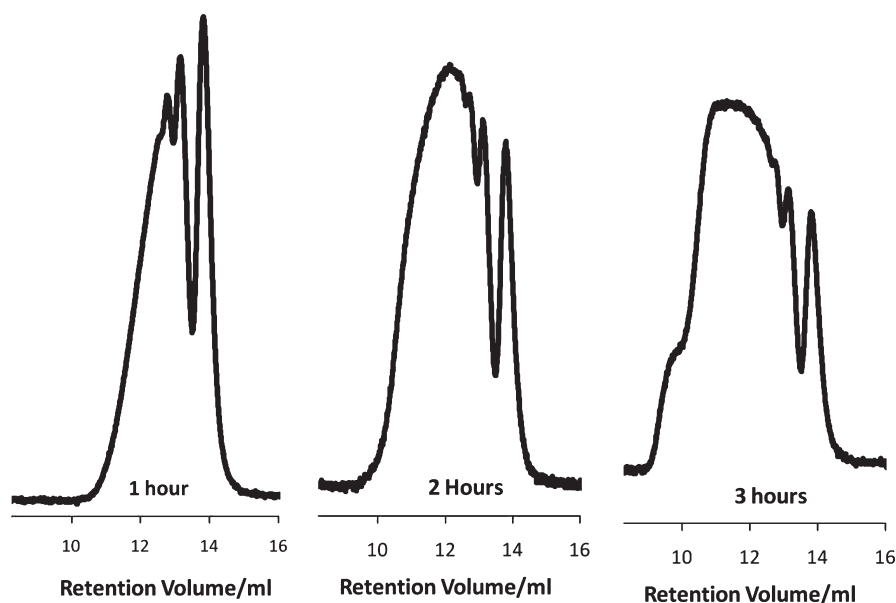


**Figure 2.** SEC chromatograms for synthesis of polybutadiene HyperMac from PB2 ( $M_n$  15 750 g mol<sup>-1</sup>) after various times. Coupling reaction carried out at 60 °C, 50:50 DMAc/THF.

**Table 4.** Molecular Weight, Polydispersity, and Intrinsic Viscosity Data for the Synthesis of PMMA HyperMacs from Macromonomers PMMA1 and PMMA2 at 40 and 80 °C

	temp/°C	$M_n$ /g mol <sup>-1</sup>	$Dp_n$	$M_w$ /g mol <sup>-1</sup>	$Dp_w$	PDI	$[\eta]_{\text{hyper}}/\text{dL g}^{-1}$ <sup>a</sup>	$[\eta]_{\text{linear}}/\text{dL g}^{-1}$ <sup>b</sup>	$g'$ <sup>c</sup>
PMMA1	40	26 400	2.4	64 400	5.5	2.4	0.18	0.22	0.78
PMMA1	80	34 000	3.0	88 400	7.5	2.6	0.21	0.28	0.75
PMMA2	40	104 800	3.4	258 300	8.1	2.5	0.42	0.59	0.71
PMMA2	80	315 300	10.3	1 680 000	53.0	5.3	0.77	2.3	0.33

<sup>a</sup> Measured by SEC viscometry. <sup>b</sup> Calculated using the Mark–Houwink equation  $[\eta] = KM^a$ . <sup>c</sup>  $g' = [\eta]_{\text{hyper}}/[\eta]_{\text{linear}}$ .

hydrodynamic volume and are more compact than linear polymers of identical molecular weight; they therefore have relatively lower intrinsic viscosities. As the reaction proceeds, the values of  $[\eta]_{\text{hyper}}$  and  $[\eta]_{\text{linear}}$  diverge, and the value of  $g'$  decreases dramatically to values of between 0.3 and 0.4, indicating highly compact, branched structures. However, it should be noted that the values of  $g'$  should be considered with some caution since the intrinsic viscosity of the HyperMac is of a material that is polydisperse not only in molecular weight but also in molecular architecture, whereas the intrinsic viscosity of the linear polymer is calculated from the Mark–Houwink equation and therefore the value represents that of a monodisperse polymer.

A coupling reaction with PB1 macromonomer ( $M_n$  6500 g mol<sup>-1</sup>) using the same reaction conditions as those described above for PB2 resulted in a dramatic increase in the  $Dp_w$  compared to the higher molecular weight macromonomer, PB2. After 2 h the HyperMac prepared from PB1 had a  $Dp_w$  approaching 80 (corresponding to a  $M_w$  in excess of 500 000 g mol<sup>-1</sup>). Beyond this point in time accurate molecular weight data could not be obtained due to decreased HyperMac solubility in the SEC solvent THF. Samples for SEC analysis were added to THF (containing a small amount of antioxidant) and agitated for 2 weeks; however, after this time the polymer resembled a swollen gel. Similar observations of gel-like polymers have been made for polystyrene HyperMacs.<sup>41</sup> We do not believe that this particular polybutadiene HyperMac has formed an insoluble cross-linked network, but we do believe that given the high polydispersity of HyperMacs, it is inevitable that with values of  $Dp_w$  possibly well in excess of 100, it is likely that there is a VERY high molecular weight component to this HyperMac which results in this gel-like behavior. The extent of this coupling

reaction was unexpectedly high and higher than previously observed. The most likely explanation lies in the lower molecular weight of the macromonomer. As the molecular weight of the macromonomer decreases, so does the viscosity of the resulting solution, making mixing easy; viscosity as a limiting factor in these reactions has been discussed above and elsewhere.<sup>41</sup> Furthermore, since the coupling reactions in question are carried out at constant w/v concentration, a lower molecular weight macromonomer will have a higher concentration of reactive functionalities, which will also lead to an enhanced rate and extent of reaction.

**PMMA HyperMacs.** PMMA is soluble in DMF, and as such PMMA macromonomers could be coupled under the same conditions as previously used for polystyrene macromonomers, i.e., 20% w/v solution concentration in DMF with cesium carbonate as the base. Coupling reactions were carried out with macromonomers PMMA1 and PMMA2 (samples 3 and 4, Table 1) at two different temperatures, 40 and 80 °C, and the results are shown in Table 4. It is clear that both macromonomers successfully underwent coupling to form PMMA HyperMacs at both temperatures, but the extent of the coupling reactions varied. At 40 °C PMMA1, the lower molecular weight macromonomer ( $M_n$  11 200 g mol<sup>-1</sup>) coupled to a very modest extent with a  $Dp_n$  of 2.4 and a  $Dp_w$  of 5.5 after 24 h. Increasing the temperature from 40 to 80 °C resulted in a slight increase in the extent of coupling with  $Dp_n$  and  $Dp_w$  increasing to 3.0 and 7.5, respectively, and an increase in the rate of reaction, with no further increase in molecular weight being observed after 6 h. These results are relatively disappointing when compared to the data for polybutadiene and polystyrene HyperMacs, but it should be noted that <sup>1</sup>H NMR indicated that only 63% (sample 3, Table 1) of polymer chains were successfully end-capped



Table 5. Molecular Weight Data of PS-PI-PS HyperBlock<sup>a</sup>

expt	solvent <sup>b</sup>	temp/°C	conc/% w/v	$M_n$ /g mol <sup>-1 c</sup>	$Dp_n$ <sup>d</sup>	$M_w$ /g mol <sup>-1 c</sup>	$Dp_w$ <sup>d</sup>	PDI
1	DMF	20	20	65 500	1.4	137 900	2.5	2.1
2	DMF/THF	40	20	125 700	2.7	270 000	4.9	2.2
3	DMF/THF	40	10	225 400	4.9	540 100	9.9	2.4
4	DMF/THF	40	5	242 700	5.3	654 300	12.0	2.7
5	DMF/THF	50	10	545 200	11.8	1 370 000	25.2	2.5
6	DMF/THF	60	10	486 200	10.5	1 730 000	31.8	3.6
7	DMF/THF	80	10	269 900	5.9	723 700	13.3	2.7
8	DMF/THF	80	5	109 800	2.4	220 200	4.0	2.0

<sup>a</sup> The effect of solvent, temperature, and solution concentration upon the extent of reaction. <sup>b</sup> DMF/THF mixed solvent was 50/50 v/v. <sup>c</sup> Molecular weights obtained by triple detection SEC using a value of  $dn/dc$  of 0.185 — that of PS. <sup>d</sup> For the  $Dp$  calculations macromonomer molecular weight  $M_n$  46 100 and  $M_w$  54 400. Obtained by triple detection SEC using a value of  $dn/dc$  of 0.185.

with 1,3-dibromopropane. This reduced level of alkyl bromide functionality will have undoubtedly have had a major impact on the degree of coupling. In contrast, the data for PMMA2, which has a degree of end-capping of greater than 95%, are more in keeping with previous data. At 40 °C the extent of coupling after 24 h results in a  $Dp_n$  of 3.4 and a  $Dp_w$  of 8.1; however, increasing the temperature from 40 to 80 °C resulted in a significant increase in the extent of coupling with  $Dp_n$  and  $Dp_w$  increasing to 10.3 and 53.0, respectively, and once again the reaction proceeded more rapidly and the molecular weight reached a plateau after 5–6 h. In the latter case the low value of  $g'$  (0.33) indicates the highly branched nature of the resulting polymer. The intrinsic viscosity of linear polymers ( $[\eta]_{\text{linear}}$ ) of the appropriate molecular weight were calculated using the Mark-Houwink equation with  $K = 7.5 \times 10^{-5}$  dL g<sup>-1</sup> and  $a = 0.72$ .<sup>48</sup>

**Polystyrene-Polyisoprene-Polystyrene (PS-PI-PS) HyperMacs: HyperBlocks.** A series of experiments were carried out to optimize reaction conditions for the coupling of the PS-PI-PS macromonomer. The choice of solvent had to be tailored to balance solubility and dielectric constant given the fact that the polystyrene blocks are soluble in high dielectric solvents such as DMF and DMAc, whereas the polyisoprene block is insoluble in these solvents. It had been hoped that with a polystyrene content of 40% the block copolymer might be sufficiently soluble in DMF, but an attempted coupling reaction carried out in DMF at room temperature resulted in almost no coupling at all (experiment 1, Table 5). After 24 h the values of  $Dp_n$  and  $Dp_w$  were 1.4 and 2.5, respectively. This low degree of coupling was attributed to poor solubility. In order to improve the solubility, a mixed solvent of DMF and THF was used (50:50 v/v) and the temperature was raised to 40 °C. The combined effect of these changes was a modest improvement in the extent of reaction with  $Dp_n$  and  $Dp_w$  increasing to 2.7 and 4.9, respectively, after 24 h. However, these slightly improved results do not compare well to previous data for other systems, and solubility still appeared to be a problem. It could be observed visually that the polymer was not truly dissolved in the mixed solvent, and given that the solubility of the macromonomer was suboptimal at the start of the reaction, it is to be expected that this situation would be exacerbated as the molecular weight of the polymer increased. At this point we were a little reluctant to try and enhance the solubility, and therefore the extent of reaction, by simply increasing the temperature since polyisoprene is particularly susceptible to thermo-oxidative degradation. Instead, it was decided to reduce the solution concentration first to 10% and then 5% w/v. This may seem counter-intuitive since we have previously reported<sup>32</sup> that reducing the concentration results in a higher degree of intramolecular coupling at the expense of the desired intermolecular coupling and a concomitant reduction in the molecular weight of

the resulting HyperMac. However, since intramolecular cyclization reactions were also shown to be less prevalent when the molecular of the macromonomer was high (as it in this case) and given the evident effect of poor solubility upon the extent of the coupling, it was felt that any deleterious effect of dilution on the amount of intermolecular coupling might be outweighed by the beneficial effect of improved solubility. This proved to be the case. Reducing the concentration from 20% to 10% w/v resulted in an increase in  $Dp_n$  and  $Dp_w$  to 4.9 and 9.9—still below the level of coupling observed in other systems (PS, PMMA, and PB) but a significant improvement. Diluting the polymer solution concentration further to 5% led to a further improvement. Identical experiments were carried out using a mixed solvent of THF and DMAc (50/50 v/v) at 40 °C and solution concentrations of 5% and 10% w/v, but far from improving the extent of coupling reaction the results were slightly worse. In order to try and push the extent of reaction higher—toward the levels of  $Dp_n$  and  $Dp_w$  achieved in previous examples—there appeared little option but to increase the temperature. A series of experiments were therefore carried out at 50, 60, and 80 °C (experiments 5–8, Table 5). Increasing the temperature to 50 °C resulted in a dramatic increase in the extent of reaction with  $Dp_n$  and  $Dp_w$  rising to 11.8 and 25.2, respectively. The large increase in the extent of reaction was accompanied by an increase in the rate of reaction. All previous values of  $Dp_n$  and  $Dp_w$  were for coupling reactions which had proceeded for 24 h. The data quoted for the coupling reaction carried out at 50 °C were obtained from a sample extracted after 6.5 h. The vastly improved extent of the coupling reaction arises as a result of the combined effects of increased solubility and temperature. Increasing the temperature to 60 °C led to a further increase in the extent and rate of reaction with values of  $Dp_n$  and  $Dp_w$  of 10.5 and 31.8, respectively, obtained after 2 h. In both of these latter experiments the coupling reactions were allowed to proceed beyond 6.5 and 2 h, but accurate molecular weight data could not be obtained due to decreased HyperBlock solubility in the SEC solvent THF. This phenomenon was also observed during the synthesis of polybutadiene HyperMacs and has been previously reported for the synthesis of PS HyperMacs.<sup>41</sup> Raising the temperature further to 80 °C did not lead to further improvements; in fact, the opposite was observed. Coupling reactions with solution concentrations of 10% and 5% w/v were carried out at 80 °C but resulted in substantially lower degrees of coupling. We suspect that the cause of this is twofold. First, there is evidence of peak broadening to longer elution times (lower molecular weights) in the SEC chromatogram after prolonged heating at 80 °C, which is indicative of polymer degradation. Second, at this temperature the reaction is well above the boiling point of THF (65 °C), and as such it is likely that some of the THF is present as vapor and it is possible

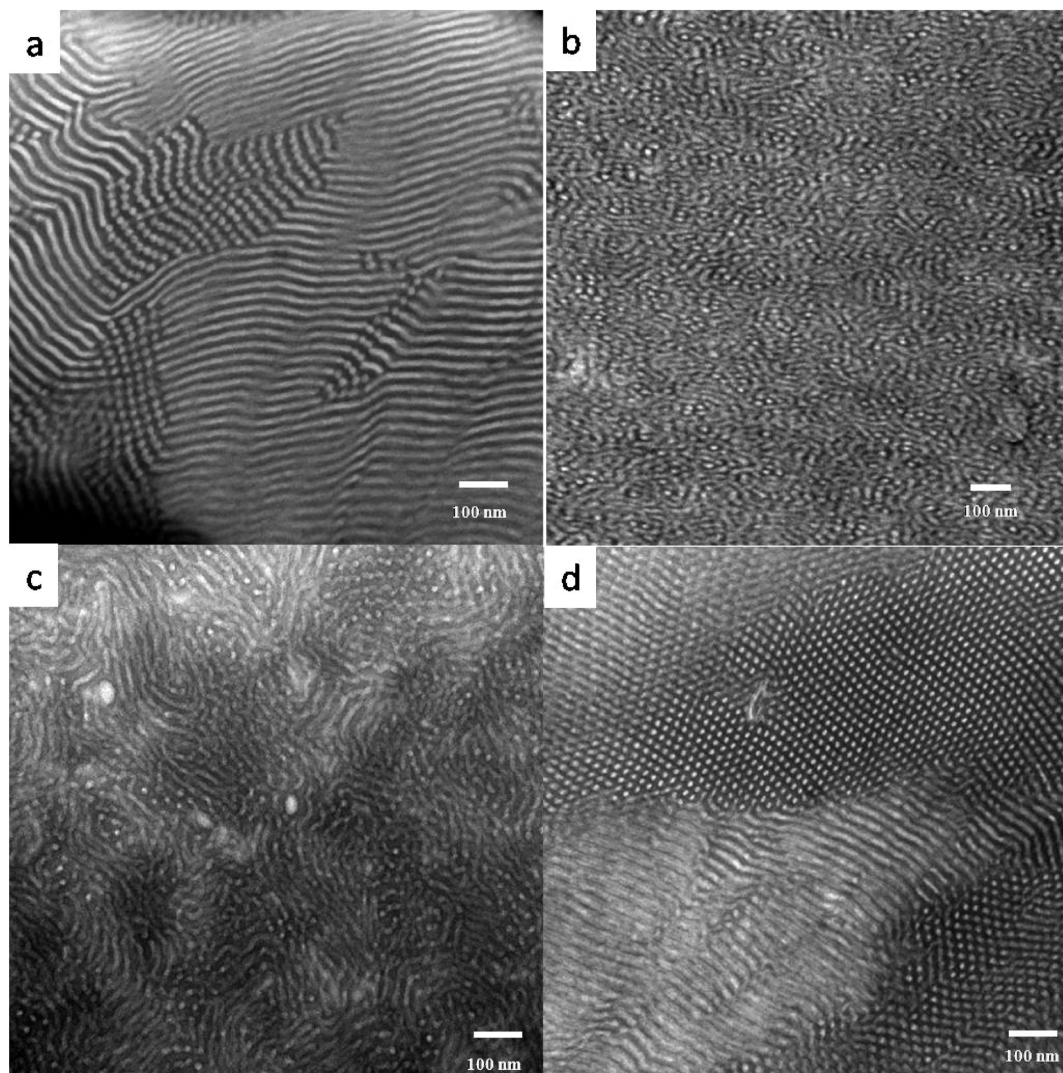


**Figure 3.** TEM micrograms of (a) PS-PI-PS macromonomer, (b) PS-PI-PS HyperBlock (H1), (c) Kraton D-1160 (K1), and (d) Kraton D-11245P (K2).

that the composition of the reaction solvent is actually less than 50/50 v/v THF/DMF. This in turn may have had a negative impact upon the polymer solubility. It is clear that solubility plays a very major part in the success or otherwise of these coupling reactions, and it would appear that the optimal conditions for the synthesis of PS-PI-PS HyperBlocks was to use a mixed solvent of THF/DMF and a temperature of 50–60 °C.

Having optimized the coupling conditions using small scale reactions (1–2 g) (Table 5), a larger scale reaction was carried out in order to provide sufficient material to allow investigations into the physical properties of HyperBlocks. Hence, 20 g of the same PS-PI-PS macromonomer was coupled as a 10% w/v solution in THF/DMF (50/50 v/v) at 60 °C. For some reason which is not immediately obvious, scaling up the reaction resulted in a lower degree of coupling, and the resulting HyperBlock had a molecular weight of 899 200 g mol<sup>-1</sup> ( $M_w$ ), a PDI of 2.9, and values of  $Dp_n$  and  $Dp_w$  of 6.7 and 16.5, respectively. It is possible that the cause of this lesser extent of reaction is due to less efficient stirring of the larger scale reaction. Nevertheless, the coupling reaction clearly did work, and the result is a highly branched PS-PI-PS HyperBlock (H1); this sample was used for all the subsequently described characterization studies.

**HyperBlocks Morphology.** In order to investigate the effect of the branched architecture upon the solid-state morphology of HyperBlock (H1) and to compare the HyperBlock morphology to commercial TPEs, we carried out transmission electron microscopy (TEM) on the HyperBlock (H1) and two commercial TPEs: Kraton D-1160 (K1), a linear PS-PI-PS triblock copolymer with a styrene content of ca. 20% and a molecular weight of  $\sim 180\,000$  g mol<sup>-1</sup>, and Kraton D-11245P (K2), a 3-arm star branched PS-PI block copolymer with a styrene content of ca. 30% and a molecular weight of 210 000 g mol<sup>-1</sup> (data supplied by Kraton). It can be clearly seen in Figure 3a that the linear PS-PI-PS macromonomer is microphase separated with a very well-defined cylindrical morphology with cylinders of polystyrene in a matrix of polyisoprene. This sample also shows a high degree of long-range order, and given the total PS content (40%) in the triblock copolymer, such a morphology is not unexpected.<sup>49</sup> However, the morphology of the HyperBlock derived from this macromonomer is dramatically different. In Figure 3b we can see that the HyperBlock is microphase separated but with no long-range order at all. In terms of composition these two samples are identical; they differ only in terms of molecular weight and molecular architecture. Although it is to be expected that the higher molecular weight HyperBlock might take longer to reach equilibrium

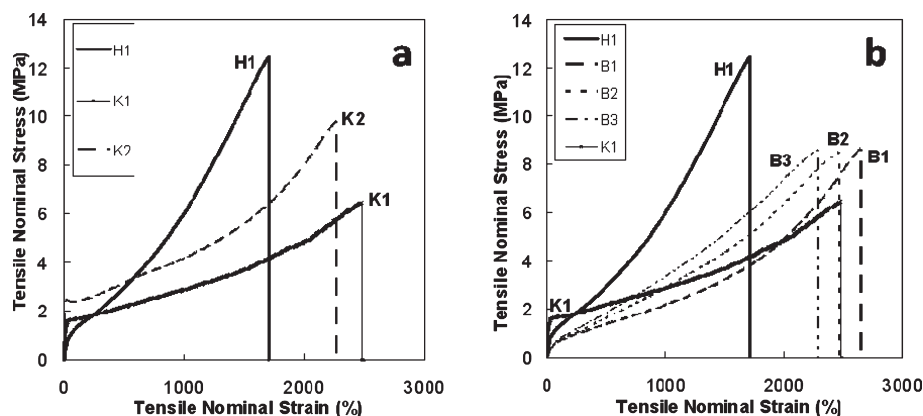


**Figure 4.** Representative tensile stress–strain behavior for (a) HyperBlock (H1), Kraton D-1160 (K1), and Kraton D-11245P (K2) and (b) HyperBlock (H1), Kraton D-1160 (K1), and blends of H1 and K1 containing 10% H1 (B1), 20% H1 (B2), and 30% H1 (B3). All tests were carried out at constant nominal strain rate of  $0.01 \text{ s}^{-1}$  and at  $20 \pm 1.5^\circ \text{C}$ .

**Table 6.** Mechanical Properties of Hyperblock (H1), Kraton D-1160 (K1), Kraton D-11245P (K2), and Blends of HyperBlock and Kraton D-1160 (B1, B2, and B3) Tested at Constant Nominal Strain Rate ( $0.01 \text{ s}^{-1}$ ) and Temperature of  $20 \pm 1.5^\circ \text{C}$

sample	Young's modulus (MPa), $E \pm \text{SD}$	tensile strength (MPa), $\sigma_{\text{UTS}} \pm \text{SD}$	strain at break (%), $\epsilon_b \pm \text{SD}$	tensile stress at intermediate strain (MPa)	
				$\sigma_{1000} \pm \text{SD}$	$\sigma_{1500} \pm \text{SD}$
H1	$3.21 \pm 0.24$	$12.39 \pm 0.79$	$1634 \pm 48.9$	$6.02 \pm 0.73$	$11.44 \pm 0.51$
K1	$11.67 \pm 0.49$	$6.09 \pm 0.71$	$2364 \pm 135.3$	$2.88 \pm 0.68$	$3.68 \pm 0.29$
K2	$23.60 \pm 0.30$	$9.42 \pm 1.26$	$2168 \pm 83.2$	$4.16 \pm 1.10$	$5.95 \pm 0.55$
B1	$0.93 \pm 0.25$	$8.45 \pm 0.93$	$2541 \pm 90.6$	$2.17 \pm 0.65$	$3.61 \pm 0.39$
B2	$0.95 \pm 0.23$	$8.42 \pm 0.85$	$2321 \pm 91.2$	$2.89 \pm 0.60$	$4.36 \pm 0.48$
B3	$1.27 \pm 0.19$	$8.61 \pm 0.83$	$2200 \pm 140.5$	$3.35 \pm 0.61$	$5.05 \pm 0.49$

morphology, we believe that the sample preparation method gives ample time for equilibration, and we suggest that it is the highly branched architecture which frustrates and inhibits any long-range order. Similar observations of disordered morphologies in highly branched multigraft copolymers have been reported in the literature.<sup>50,51</sup> The TEM of commercial linear triblock copolymer K1 (Figure 3c) also shows a clear microphase-separated morphology, but the long-range order is less well-defined. There are regions where it appears as if the morphology is cylindrical, but it is possible that at a composition of about 20% styrene, this polymer is on the cusp between cylindrical and spherical morphology, which might account for the less well-defined order. In contrast, the star-branched commercial TPE K2 (Figure 3d) shows a very well-defined long-range order and clearly shows a hexagonally packed cylindrical morphology. Although very similar to the macromonomer shown in Figure 3a, the domain sizes are noticeably different. In the case of K2 the styrene (cylindrical) domains are smaller and the polyisoprene matrix more prevalent—consistent with the lower styrene content in the latter's case.

**Mechanical Properties.** Thermoplastic elastomers (TPEs) are a tremendously useful class of polymers and derive their elastic properties from the microphase-separated morphology in which the rubbery matrix is anchored by physical cross-links formed by the glassy domains. Tensile failure of TPEs arises as a result of rupture of the glassy domains which are held together by chain entanglement. In the case of HyperBlocks at the heart of the polystyrene glassy domains are chemical covalently bonded branch points, and it is not unreasonable to suppose that the combination of chain entanglement and branch points might lead to superior mechanical properties. There have been a number of reports in the literature of highly branched TPEs. In a series of papers Mays et al.<sup>50–53</sup> describe the synthesis of multigraft copolymers and the influence of molecular architecture and

composition upon the morphology and mechanical properties. Mays described how the number and functionality of junction points impacts upon the morphology and notes that polymers with a greater number of junction points have little long-range order. He also goes on to describe the relationship between these two parameters and the mechanical properties such that strain at break and tensile strength increased linearly with the number of junction points per molecule and that tetrafunctional multigraft copolymers showed a surprisingly high strain at break, far exceeding that of commercial block copolymer thermoplastic elastomers (TPEs). The relationship between styrene content in tetrafunctional multigraft copolymers and mechanical properties was investigated,<sup>53</sup> and generally the materials became less elastic and more plastic as the styrene content increased from 8% to 67%. This is to be expected given the change in morphology accompanying the change in composition. However, a sample with 22% styrene had an anomalously high tensile strength and high strain at break. This behavior was attributed to a wormlike cylindrical morphology with little long-range order. In another study Puskas et al.<sup>54,55</sup> describe the synthesis and characterization of dendritic block copolymers with a highly branched core of polyisobutylene and a periphery of glassy polymer such as polystyrene or poly(*p*-methylstyrene). They too show promising properties as TPEs although the relationship between mechanical properties and styrene content is more predictable than the work described by Mays. More intriguingly, the same group have recently reported<sup>56</sup> the synthesis and characterization of analogous dendritic copolymers with a polyisobutylene core and short copolymer end sequences which exhibit TPE properties regardless of the  $T_g$  of the end sequences. Such materials included copolymers of isobutylene with isoprene, *p*-methylstyrene, and cyclopentadiene.

In order to investigate the mechanical properties of HyperBlocks and to compare the HyperBlock properties to



commercial TPEs, we carried out a series of tests on the HyperBlock (H1) and the two commercial TPEs, K1 and K2. Blends of H1 and K1 containing 10% H1 (B1), 20% H1 (B2), and 30% H1 (B3) were also prepared and tested. Tensile testing on H1, K1, K2, B1, B2, and B3 used the same specimen geometry at constant nominal strain rate and revealed some very interesting results. It can be seen from the data in Figure 4a and Table 6 that the ultimate tensile strength (UTS) of H1 (average UTS of 12.39 MPa) compares favorably with and indeed exceeds the UTS of the two commercial TPEs K1 and K2, which have an average UTS of 6.09 and 9.42 MPa, respectively. H1 however shows a lower strain at break than both K1 and K2 with average values of 1634%, 2364%, and 2168%, respectively. It could be argued that the trend in results for H1, K1, and K2 can be explained solely by the change in styrene content. Indeed, ordinarily one would expect such a trend of increasing tensile strength and lower strain at break to accompany an increase in polystyrene content as the expected morphology changes from spherical domains of PS through hexagonally packed cylinders toward a more lamellae-like morphology. However, it is clear from the TEM data in Figure 3b that the highly branched architecture of the HyperBlock frustrates the formation of any long-range order in the morphology, and the relationship between composition and mechanical properties is not so obvious. However, we do not have sufficient data from this single sample of HyperBlock to expand further. Work is in progress to synthesize a library of HyperBlocks with a distribution of compositions to investigate further the relationship between architecture, composition, and mechanical properties. Although the ultimate properties at failure (UTS and strain at break) are of great significance, it is also worth looking at the behavior at intermediate strains. The commercial TPEs K1 and K2 show very sharp yield points with high values of yield stress and Young's modulus, whereas H1 has a softer yield and much lower yield stress and Young's modulus. It has been reported<sup>50</sup> that a low Young's modulus is desirable for the successful application of thermoplastic elastomers. In addition to H1 having a lower Young's modulus and yield stress than the commercial TPEs, at intermediate strains (1000% and 1500%) the tensile stress of H1 far exceeds that of K1 and K2.

Perhaps of more interest is the behavior of the blends. With the addition of 10% H1 to K1 to give blend B1 we can see dramatically different mechanical properties. Intriguingly, we see in Figure 4b and Table 6 that the blend B1 has a higher elongation at break and a higher ultimate tensile stress with the former increasing by about 7.5% and the UTS increasing by nearly 40% in comparison to K1. To observe an increase in both properties was most unexpected. Furthermore, B1 shows a substantially lower yield stress and Young's modulus than both of the constituent polymers H1 and K1. B1 has a Young's modulus which is more than an order of magnitude lower than K1! It seems inconceivable that these dramatic changes have anything to do with a change in polystyrene content since the PS content in the blend B1 is only 2% higher than that of K1. Furthermore, H1 has  $M_w$  900 kg mol<sup>-1</sup> and  $M_n$  310 kg mol<sup>-1</sup>, substantially higher than that of K1 (~180 kg mol<sup>-1</sup>); however, it has been reported that the mechanical properties of TPEs do not show a strong dependence on molecular weight<sup>50</sup> in excess 100 kg mol<sup>-1</sup>. It would therefore seem likely that the blending of the HyperBlock into the linear commercial TPE K1 has enhanced the mechanical properties as a result of its molecular architecture rather than its molecular weight or composition. Unfortunately, we had insufficient samples of B1 to go back

and look at the effect of adding 10% H1 on the morphology of K1. The addition of greater amounts of H1 to give blends B2 (20% H1) and B3 (30% H1) resulted in samples with very similar UTS to B1 and a slightly reduced elongation at break. However, although the UTS values in B2 and B3 were nearly identical to B1, the tensile stress at intermediate strains increased with increasing amounts of H1. The yield stress and Young's modulus similarly increased with increasing amounts of H1. It is not immediately obvious how H1 so dramatically modifies the properties of K1, and it is most intriguing that the blend B1 does *not* display properties intermediate between the constituent polymers H1 and K1 but shows enhanced stress at high strain and a significantly reduced yield stress and Young's modulus.

## Conclusions

We have demonstrated the versatility of the "macromonomer" approach by describing modified strategies for the synthesis of AB<sub>2</sub> macromonomers of polybutadiene, poly(methyl methacrylate), and ABA triblock copolymers of polystyrene–polyisoprene–polystyrene via living anionic polymerization. We have also described the conversion of the linear macromonomers into the highly branched HyperMacs via a Williamson coupling reaction in which the solvent and temperature have to be optimized in each case. Furthermore, we have investigated both the solid-state morphology and mechanical properties of the highly branched block copolymers—known from here on in as HyperBlocks—and considered their properties in comparison to two commercial available thermoplastic elastomers. We have shown that although HyperBlocks undergo microphase separation in the solid state, their highly branched architecture frustrates the formation of any long-range order in the morphology. This absence of long-range order does not appear to inhibit the mechanical properties, and the HyperBlock has tensile properties that compare well to the commercial TPEs. Also of significant interest is the effect of the addition of small quantities of HyperBlock on the mechanical properties of the commercial TPE K1. Rather than displaying properties which are intermediate between the constituent polymers H1 and K1, blend B1 containing 10% of HyperBlock shows enhanced stress at high strain, a greater elongation at break, and ultimate tensile stress coupled with a significantly reduced yield stress and Young's modulus. These results were most unexpected, and although we have insufficient data at present to fully explain these phenomena, work is about to commence on a program to synthesize a library of HyperBlocks in which we will investigate the relationship between HyperBlock composition, architecture, and blend composition upon phase-separated morphology and mechanical properties.

**Acknowledgment.** This work was financially supported by the Engineering and Physical Sciences Research Council and the Department of Chemistry, Durham University. We also thank Dr Sergio Corona Galvan, Repsol YPF for the supply of samples of InitiaLi 103 and Dr Noël De Keyser, Kraton Polymers for the supply of commercial thermoplastic elastomers.

## References and Notes

- (1) Adams, C. H.; Hutchings, L. R.; Klein, P. G.; McLeish, T. C. B.; Richards, R. W. *Macromolecules* **1996**, *29*, 5717–5722.
- (2) Grest, G. S.; Fetters, L. J.; Huang, J. S.; Richter, D. *Adv. Chem. Phys.* **1996**, *94*, 67–163.
- (3) Clarke, N.; Colley, F. R.; Collins, S. A.; Hutchings, L. R.; Thompson, R. L. *Macromolecules* **2006**, *39*, 1290–1296.
- (4) Hutchings, L. R.; Richards, R. W. *Polym. Bull.* **1998**, *41*, 283–289.
- (5) Hutchings, L. R.; Richards, R. W. *Macromolecules* **1999**, *32*, 880–891.

- (6) Iatrou, H.; Hadjichristidis, N. *Macromolecules* **1993**, *26*, 2479–2484.
- (7) Roovers, J.; Toporowski, P. M. *Macromolecules* **1981**, *14*, 1174–1178.
- (8) Hakiki, A.; Young, R. N.; McLeish, T. C. B. *Macromolecules* **1996**, *29*, 3639–3641.
- (9) Chalari, I.; Hadjichristidis, N. *J. Polym. Sci., Part A: Polym. Chem.* **2002**, *40*, 1519–1526.
- (10) Orfanou, K.; Iatrou, H.; Lohse, D. J.; Hadjichristidis, N. *Macromolecules* **2006**, *39*, 4361–4365.
- (11) Matmour, R.; Gnanou, Y. *J. Am. Chem. Soc.* **2008**, *130*, 1350–1361.
- (12) Lepoittevin, B.; Matmour, R.; Francis, R.; Taton, D.; Gnanou, Y. *Macromolecules* **2005**, *38*, 3120–3128.
- (13) Angot, B.; Taton, D.; Gnanou, Y. *Macromolecules* **2000**, *33*, 5418–5426.
- (14) Trollsas, M.; Hedrick, J. L. *J. Am. Chem. Soc.* **1998**, *120*, 4644–4651.
- (15) Hirao, A.; Sugiyama, K.; Tsunoda, Y.; Matsuo, A.; Watanabe, T. *J. Polym. Sci., Part A: Polym. Chem.* **2006**, *44*, 6659–6687.
- (16) Matsuo, A.; Watanabe, T.; Hirao, A. *Macromolecules* **2004**, *37*, 6283–6290.
- (17) Hirao, A.; Matsuo, A.; Watanabe, T. *Macromolecules* **2005**, *38*, 8701–8711.
- (18) Deffieux, A.; Schappacher, M.; Hirao, A.; Watanabe, T. *J. Am. Chem. Soc.* **2008**, *130*, 5670–5672.
- (19) Hirao, A.; Watanabe, T.; Ishizu, K.; Ree, M.; Jin, S.; Jin, K. S.; Deffieux, A.; Schappacher, M.; Carlotti, S. *Macromolecules* **2009**, *42*, 682–693.
- (20) Urbani, C. N.; Bell, C. A.; Whittaker, M. R.; Monteiro, M. J. *Macromolecules* **2008**, *41*, 1057–1060.
- (21) Urbani, C. N.; Bell, C. A.; Lonsdale, D.; Whittaker, M. R.; Monteiro, M. J. *Macromolecules* **2008**, *41*, 76–86.
- (22) Whittaker, M. R.; Urbani, C. N.; Monteiro, M. J. *J. Am. Chem. Soc.* **2006**, *128*, 11360–11361.
- (23) Hutchings, L. R.; Roberts-Bleming, S. J. *Macromolecules* **2006**, *39*, 2144–2152.
- (24) Kimani, S. M.; Hutchings, L. R. *Macromol. Rapid Commun.* **2008**, *29*, 633–637.
- (25) Teertstra, S. J.; Gauthier, M. *Prog. Polym. Sci.* **2004**, *29*, 277–327.
- (26) Muchtar, Z.; Schappacher, M.; Deffieux, A. *Macromolecules* **2001**, *34*, 7595–7600.
- (27) Schappacher, M.; Deffieux, A.; Putaux, J. L.; Viville, P.; Lazzaroni, R. *Macromolecules* **2003**, *36*, 5776–5783.
- (28) Bernard, J.; Schappacher, M.; Viville, P.; Lazzaroni, R.; Deffieux, A. *Polymer* **2005**, *46*, 6767–6776.
- (29) Tomalia, D. A.; Hedstrand, D. M.; Ferritto, M. S. *Macromolecules* **1991**, *24*, 1435–1438.
- (30) Gauthier, M.; Moller, M. *Macromolecules* **1991**, *24*, 4548–4553.
- (31) Puskas, J. E.; Grasmuller, M. *Macromol. Symp.* **1998**, *132*, 117–126.
- (32) Hutchings, L. R.; Dodds, J. M.; Roberts-Bleming, S. J. *Macromolecules* **2005**, *38*, 5970–5980.
- (33) Knauss, D. M.; Al-Muallem, H. A. *J. Polym. Sci., Part A: Polym. Chem.* **2000**, *38*, 4289–4298.
- (34) Knauss, D. M.; Al-Muallem, H. A.; Huang, T. Z.; Wu, D. T. *Macromolecules* **2000**, *33*, 3557–3568.
- (35) Bender, J. T.; Knauss, D. M. *Macromolecules* **2009**, *42*, 2411–2418.
- (36) Lopez-Villanueva, F. J.; Wurm, F.; Kilbinger, A. F. M.; Frey, H. *Macromol. Rapid Commun.* **2007**, *28*, 704–709.
- (37) Wurm, F.; Lopez-Villanueva, F. J.; Frey, H. *Macromol. Chem. Phys.* **2008**, *209*, 675–684.
- (38) Milkovich, R.; Chaing, M. T. US Patent 3786116, **1974**.
- (39) Roos, S. G.; Muller, A. H. E.; Matyjaszewski, K. *Macromolecules* **1999**, *32*, 8331–8335.
- (40) Koutalas, G.; Iatrou, H.; Lohse, D. J.; Hadjichristidis, N. *Macromolecules* **2005**, *38*, 4996–5001.
- (41) Clarke, N.; De Luca, E.; Dodds, J. M.; Kimani, S. M.; Hutchings, L. R. *Eur. Polym. J.* **2008**, *44*, 665–676.
- (42) Dodds, J. M.; De Luca, E.; Hutchings, L. R.; Clarke, N. *J. Polym. Sci., Part B: Polym. Phys.* **2007**, *45*, 2762–2769.
- (43) Quirk, R. P.; Wang, Y. C. *Polym. Int.* **1993**, *31*, 51–59.
- (44) Quirk, R. P.; Lee, B. *Macromol. Chem. Phys.* **2003**, *204*, 1719–1737.
- (45) Hsieh, L. H.; Quirk, R. P. In *Anionic Polymerization, Principles and Practical Applications*; Marcel Dekker: New York, 1996.
- (46) Kim, C.; Morel, M. H.; Sainte Beuve, J.; Guilbert, S.; Collet, A.; Bonfils, F. *J. Chromatogr., A* **2008**, *1213*, 181–188.
- (47) Yan, X. H.; Liu, G. J. *Langmuir* **2004**, *20*, 4677–4683.
- (48) Brandrup, J.; Immergut, E. H.; Grulke, E. A.; Bloch, D. *Polymer Handbook*; Wiley-Interscience: New York, 1999.
- (49) Matsen, M. W. *J. Chem. Phys.* **2000**, *113*, 5539–5544.
- (50) Beyer, F. L.; Gido, S. P.; Buschl, C.; Iatrou, H.; Uhrig, D.; Mays, J. W.; Chang, M. Y.; Garetz, B. A.; Balsara, N. P.; Tan, N. B.; Hadjichristidis, N. *Macromolecules* **2000**, *33*, 2039–2048.
- (51) Zhu, Y. Q.; Burgaz, E.; Gido, S. P.; Staudinger, U.; Weidisch, R.; Uhrig, D.; Mays, J. W. *Macromolecules* **2006**, *39*, 4428–4436.
- (52) Uhrig, D.; Mays, J. W. *Macromolecules* **2002**, *35*, 7182–7190.
- (53) Weidisch, R.; Gido, S. P.; Uhrig, D.; Iatrou, H.; Mays, J.; Hadjichristidis, N. *Macromolecules* **2001**, *34*, 6333–6337.
- (54) Puskas, J. E.; Dos Santos, L.; Kaszas, G. *J. Polym. Sci., Part A: Polym. Chem.* **2006**, *44*, 6494–6497.
- (55) Puskas, J. E.; Kwon, Y.; Antony, P.; Bhowmick, A. K. *J. Polym. Sci., Part A: Polym. Chem.* **2005**, *43*, 1811–1826.
- (56) Puskas, J. E.; Dos Santos, L. M.; Kaszas, G.; Kulbaba, K. J. *J. Polym. Sci., Part A: Polym. Chem.* **2009**, *47*, 1148–1158.